CSS Antimony Selenide Film Morphology and High Efficiency PV Devices

Oliver S. Hutter,* Laurie J. Phillips, Peter J. Yates, Jonathan D. Major, and Ken Durose

Stephenson Institute for Renewable Energy, University of Liverpool, Liverpool, L3 5TR, United Kingdom
*ohutter@liverpool.ac.uk

***Abstract* — Knowledge of close-space sublimation (CSS) Sb_2Se_3 growth conditions is vital for proper understanding of PV performance, and optimization of Sb_2Se_3 devices. In this work, various growth parameters have been studied and the resulting Sb_2Se_3 films have been characterized using SEM, XRD and optical transmission measurements, thus illustrating the desired properties for high device performance. PV devices were fabricated using TiO_2 as a window layer combined with P3HT or PTB7 as the hole transport material, resulting in V_{oc}= 0.42 V, J_{sc}= 33.4 mAcm^{-2}, *FF*= 43.2% and *PCE*= 6.06% for P3HT.**

***Index Terms* — Antimony selenide, CSS, PV, Solar cells, thin film**

I. Introduction

Recently there has been a drive in research effort towards low cost, low toxicity, earth abundant photovoltaic (PV) absorber materials for future terawatt scale energy production. Antimony selenide (Sb_2Se_3) has seen increasing interest as a new absorber material for solar cell applications for these reasons, in addition to its suitable band gap of around 1.2 eV and high absorption coefficient of >10^5 cm^{-1}.[1],[2] The peak reported efficiency has increased from 3.2% to 6.5% in just 3 years.[3],[4] This may appear modest in comparison to other more established PV technologies, but it is impressive given that there are fewer than 100 papers with functional devices published to date. Sb_2Se_3 has an interesting orthorhombic crystal structure comprising of 1 dimensional covalently bonded ribbons, with weak van der Waals interactions holding these ribbons together and yielding potentially benign grain boundaries.[5]-[7] Consequently, the conduction of a given Sb_2Se_3 film is anisotropic, *i.e.* dependent on the crystal orientation of these ribbons. Ribbons that are aligned perpendicular to the substrate are preferred for efficient charge extraction.[6]

Sb_2Se_3 has been deposited for thin film PV applications via a variety of methods including electrodeposition,[4] chemical bath deposition,[8] and thermal evaporation.[9],[10] Close-space sublimation (CSS) has a range of advantages over other methods: it is industrially scalable, simple to implement, does not rely on high vacuum and offers high rates of deposition with significant scope for tuning conditions such as substrate temperature, source temperature, gas flow and pressure.[11]-[13]

Previous Sb_2Se_3 based devices have mostly used the ubiquitous CdS window layer from CdTe and CIGS photovoltaics. The current world record device combines a CdS window layer with a PbS quantum dot hole transport material (HTM).[4] However, CdS causes parasitic absorption, can be prone to interdiffusion, and introduces toxic Cd.[7],[14] Alternative window layers such as TiO_2 are therefore being investigated and have been reported in combination with poly(3-hexylthiophene) (P3HT) as the HTM, as depicted in Fig. 1.[12],[15]

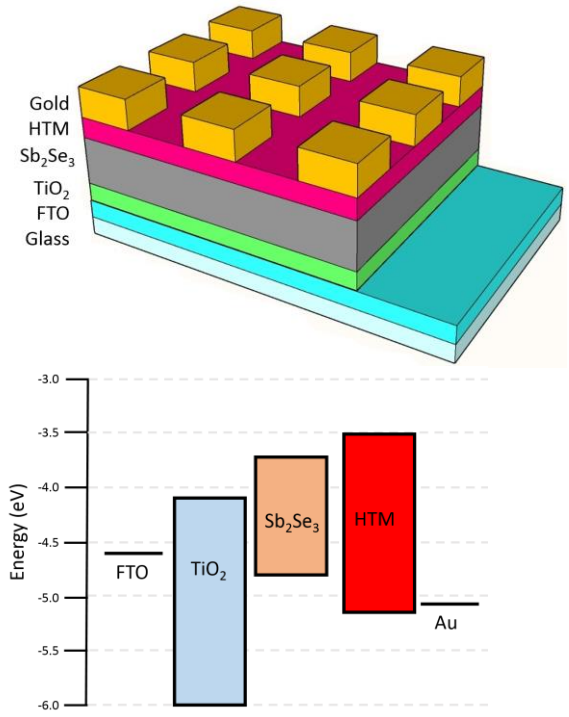

Fig. 1. Top: Schematic of material layers in Sb_2Se_3 PV devices. Bottom: Energy level diagram of the materials used in this work.

CSS growth conditions have a significant impact on the crystal structure, grain size and surface coverage of Sb_2Se_3. Moreover, the properties of the HTM affect the charge extraction in addition to blocking shunting pathways. This work investigates an alternative HTM to P3HT and studies CSS growth conditions, which is key to improving and understanding device performance more thoroughly.

In the schematic diagram of the device shown in Fig. 1, an ideal HTM would have a valence band or HOMO of the correct energy to accept a hole from the valence band of Sb_2Se_3. This should be combined with an electron affinity value smaller than the conduction band level of Sb_2Se_3. This is important to combine efficient charge transfer of any photo-generated electrons in the HTM layer over to the Sb_2Se_3, whilst blocking any movement of photo generated minority carriers from the Sb_2Se_3 to the HTM. Although these materials have previously been described merely as HTMs, there is a possibility that they may be able to contribute to the photocurrent in the device in certain circumstances.

II. Experimental

TEC10 fluorine doped tin oxide (FTO) substrates (Pilkington, UK) were cleaned sequentially in water, acetone and IPA, and UV/O_3 treated for 10 mins. The cleaned substrates were spin coated with 0.15 mol dm^{-3} and 0.3 mol dm^{-3} titanium isopropoxide in ethanol at 3000 rpm for 30s and then dried at 120˚C under N_2 for 10 mins after each of the two deposition steps. The substrates were then annealed in air at 550˚C for 30 minutes and cooled rapidly to form compact titania layers.[16] For Sb_2Se_3 CSS deposition, the substrate was preheated for 15 mins at 260 mbar and 350˚C source and substrate temperatures. Film *i* (Table 1) had different preheating conditions utilizing source and substrate temperatures of 350˚C and 390˚C respectively. Sb_2Se_3 deposition was then carried out at 13 mbar of N_2, with varying source and substrate temperatures. Specific deposition conditions for each film are listed in Table 1.

P3HT was dissolved in dichlorobenzene at a concentration of 10 mg/mL by heating at 70˚C for 1 hour, filtered through a 0.45 µm PTFE filter, and then spun cast onto Sb_2Se_3 substrates dynamically at 1000 rpm for 10 s followed by 4000 rpm for 30 s. Poly({4,8-bis[(2-ethylhexyl)oxy]benzo[1,2-b:4,5-b′]dithiophene-2,6-diyl} {3-fluoro-2-[(2-ethylhexyl)carbonyl] thieno[3,4-b] thiophenediyl}) (PTB7) was dissolved in dichlorobenzene at a concentration of 10 mg/mL by heating at 50˚C for 2 hours in air, and then spun cast onto Sb_2Se_3 substrates dynamically at 1000 rpm for 60 s. Cells were completed by thermally evaporating 100 nm of gold through a shadow mask to create cells with an active area of 0.1 cm^2 (Fig. 1).

Thickness values were measured using an Ambios Technology XP-200 surface profiler, X-ray diffraction (XRD) measurements were carried out using a Rigaku Smartlab X-ray diffractometer and scanning electron microscopy (SEM) images were taken using a JEOL 7001 FEGSEM. Transmission measurements were made using a Shimadazu SolidSpec-3700 UV-Vis Spectrophotometer. JV measurements were made under AM1.5 conditions using a calibrated TS Space Systems AAA100 solar simulator.

III. Results and Discussion

Fig. 2 shows the optical transmission of Sb_2Se_3 films deposited under different CSS conditions. Film transmission decreases as the deposition temperature and time increases, and is consistent with the films being thicker, as expected.

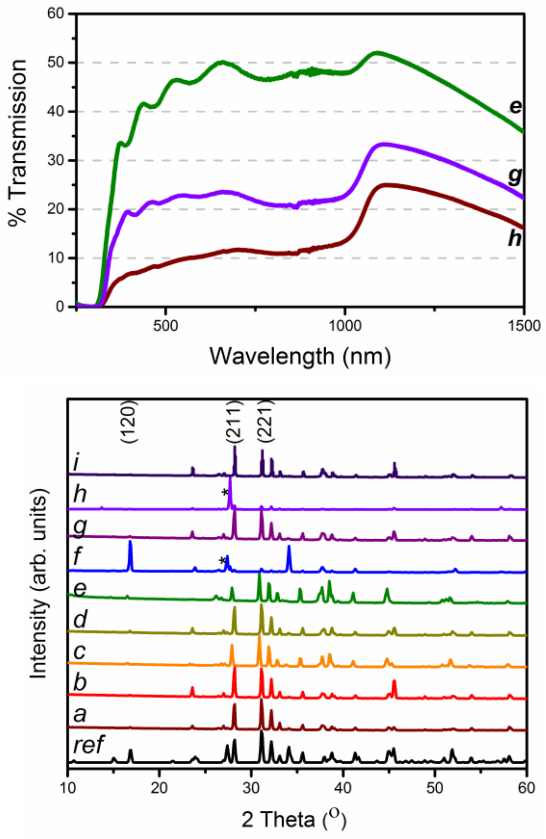

Fig. 2. Top: Optical transmission of Sb_2Se_3 films *e*, *g* and *h* grown on FTO glass with differing CSS conditions. Bottom: XRD patterns of Sb_2Se_3 films grown by CSS. Literature data for Sb_2Se_3 is shown at the bottom, with the films *a* to *i* (Table 1) shown sequentially to the top. * Denotes a peak arising from the FTO substrate.

XRD showed all Sb_2Se_3 films to have the expected orthorhombic structure, (JCPDS card no. 15-0861) however there are differences in crystallographic texture between them. For example, film *f* has a strong peak around 17˚ which is indicative of the Sb_2Se_3 ribbons lying parallel to the surface (120). This is corroborated by the SEM image of the film shown in Fig. 3f. As mentioned previously, ribbons lying parallel to the surface are unlikely to yield high device performance due to film conduction issues. Some films shown in Fig. 2 also exhibit FTO peaks in the XRD patterns, as expected due to incomplete coverage (marked * in films *f* and *h*). These areas of incomplete coverage or pinholes drastically reduce the performance in a device as they act as shunting pathways. The preferential orientation of these ribbons is perpendicular to the substrate, and this is shown with XRD peaks at 28˚ at 31˚ for (211) and (221)

TABLE I
CSS DEPOSITION CONDITIONS

	Sb_2Se_3 CSS Conditions				Peak *PCE*		
Film	Source/ ˚C	Substrate/ ˚C	Time/ m	Thickness/ µm	No HTM	P3HT	PTB7
a	440	410	45	2.7	0.30%	0.22%	-
b	450	Off	45	6.3	0%	0.38%	-
c	450	420	30	3.9	2.45%	2.66%	1.33%
d	450	420	45	6.1	0.25%	0.99%	1.18%
e	450	430	30	1.1	0%	0.37%	2.21%
f	460	430	15	2.4	0.34%	0.71%	-
g	460	430	30	3.6	1.50%	0.88%	0.98%
h	460	430	60	10.5	0.56%	0.99%	-
i	450	Off	30	2.0	3.48%	6.06%	3.90%

respectively.[6],[17],[18] These peaks correspond to the Sb_2Se_3 ribbons lying slightly tilted and vertically orientated on the surface respectively, both of which are desirable for optimal device performance.[6],[7]

Table 1 gives the thickness values for the films *a* to *i*, measured using a surface profiler. These values show that film thickness increases with increased source temperature, decreased substrate temperature and increased time, in agreement with the transmission measurements.

Table 1 shows the peak efficiencies for PV devices made with P3HT and PTB7 HTMs and with varying CSS deposition conditions, thus demonstrating how highly sensitive device performance is to each parameter. The large variance in *PCE* is due to differing source and substrate temperatures during CSS deposition combined with different deposition times producing varying Sb_2Se_3 orientations, densities and thicknesses of absorbing layers (Fig.3 and Table 1). Some films (e.g. film *h*), would be too thick to perform well in devices, as the device series resistance would be too high for efficient charge extraction.

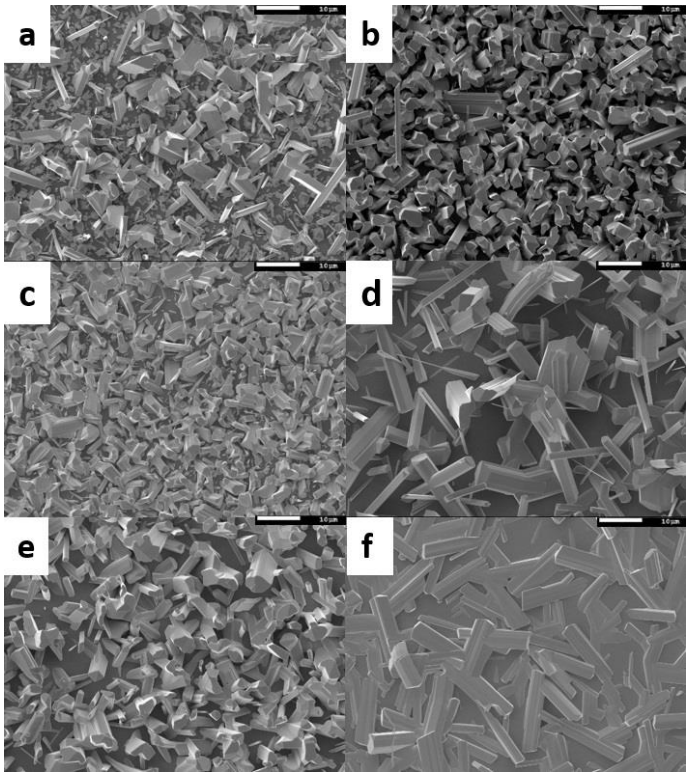

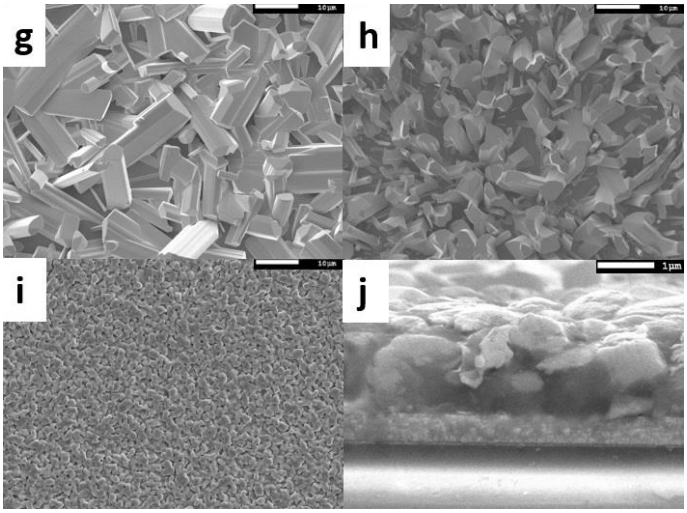

Fig. 3. SEM images of Sb_2Se_3 films deposited via CSS. Images *a* to *i* correspond to the conditions in Table 1. SEM image *j* is a cross section of a device produced in this work (film *i*). All scale bars are 10µm except for *j*, where the scale bar is 1µm.

The SEM images in Fig. 3 show that the deposited CSS films comprise rod-like grains on the scale of 10s of microns, with a large difference in grain size between the films. The voids on some of the deposited films (e.g. film *d*) explain the lower performance observed with many pixels on a device short circuiting or giving low fill factors. In common with work on CdTe, the use of spun polymer HTM and contact layer films can act to block pinholes[19] – for example, microscopy indicated that the coverage of films *b* and *e* by P3HT and PTB7 was responsible for the increase in performance from the 0% seen for the control samples. It also clear from Fig. 3 that vertically aligned Sb_2Se_3 rods are not enough for high *PCE* (e.g. film *b*), even when combined with a pinhole blocking HTM. Fig. 3*i* and *j* show how the best film (*i*) has good coverage and a much higher density of Sb_2Se_3 structures which are mostly aligned perpendicular to the substrate in a compact array, and this is reflected in the high *PCE* (Table 1). It also demonstrates that the grains in film *i* are actually smaller than in some other lesser performing films (e.g. films *f* and *g*). However, Fig. 3 also shows that in film *i*, some pinholes remain, demonstrating that these films could be optimized further to improve the *PCE*.

Table 1 shows that an Sb_2Se_3 thickness of approximately 2µm yields favorable device performance. It also demonstrates that for a more compact and smooth grain structure (film *i*), the layers are thinner compared to a similarly deposited film (Table 1) with a very different grain structure (film *b*).

Fig. 4 shows the peak cell performance for Sb_2Se_3 film *i* with P3HT as the HTM. A device cross section is also shown in Fig. 3j, demonstrating the Sb_2Se_3 grains spanning the active layer of the device from TiO_2 to HTM/Au.

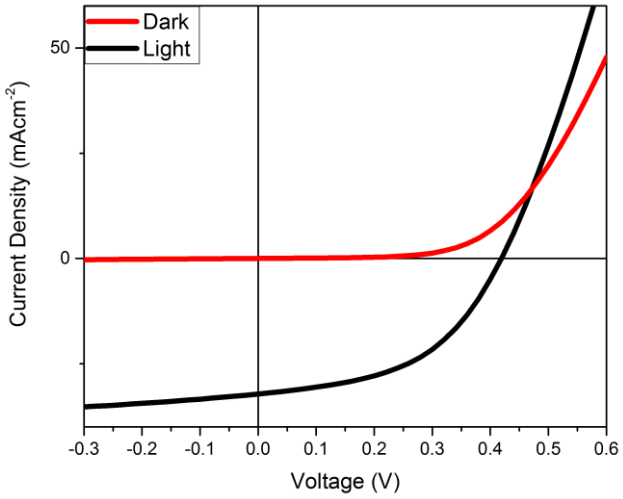

Fig. 4. Peak Sb_2Se_3 device performance (film *i*, with a P3HT HTM), with *PCE*= 6.06%, V_{oc}= 0.42 V, J_{sc}= 33.4 mAcm^{-2}, and *FF*= 43.2%.

IV. Conclusion

This work has demonstrated the sensitivity of the crystal texture and device performance of Sb_2Se_3 absorber layers to growth conditions during CSS growth. Careful optimization of preheating and deposition conditions has enabled the growth of a high density of vertically aligned, compact Sb_2Se_3 grains. By tuning the deposition conditions and by the use of P3HT as an HTM, a *PCE* of 6.06% has been achieved which is comparable to present world record devices[7] for Sb_2Se_3 within the usual experimental error for device measurement. PTB7 was investigated as a HTM, but yielded lower PCE values than P3HT. The work is ongoing and preliminary results suggest that higher *PCE* values are achievable using alternative HTM materials.

Acknowledgements

This work was supported by EPSRC grants EP/N014057/1 and EP/M024768/1. Theodore Hobson is gratefully acknowledged for his helpful discussions.

References

[1] Y. Lai, Z. Chen, C. Han, L. Jiang, F. Liu, J. Li, and Y. Liu, "Preparation and characterization of Sb_2Se_3 thin films by electrodeposition and annealing treatment," *Appl. Surf. Sci.*, *261*, 510, 2012.

[2] X. Liu, C. Chen, L. Wang, J. Zhong, M. Luo, J. Chen, and D. Xue, "Improving the performance of Sb_2Se_3 thin film solar cells over 4% by controlled addition of oxygen during film deposition," *Progress in Photovoltaics: Research and Applications*, 1828–1836, 2015.

[3] Y. C. Choi, T. N. Mandal, W. S. Yang, Y. H. Lee, and S. H. Im, "Sb_2Se_3 -sensitized inorganic–organic heterojunction solar cells fabricated using a single-source precursor," *Angewandte Chemie*, 1329, 2014.

[4] C. Chen, L. Wang, L. Gao, D. Nam, D. Li, K. Li, Y. Zhao, C. Ge, H. Cheong, H. Liu, H. Song, and J. Tang, "6.5% certified efficiency Sb_2Se_3 solar cells using PbS colloidal quantum dot film as hole-transporting layer," *ACS Energy Lett.*, *2*, 2125, 2017.

[5] Y. Zhou, M. Leng, Z. Xia, J. Zhong, H. Song, X. Liu, B. Yang, J. Zhang, J. Chen, K. Zhou, J. Han, Y. Cheng, and J. Tang, "Solution-processed antimony selenide heterojunction solar cells," *Adv. Energy Mater.*, vol. 4, no. 8, pp. 4–11, 2014.

[6] Y. Zhou, L. Wang, S. Chen, S. Qin, X. Liu, J. Chen, D.- J. Xue, M. Luo, Y. Cao, Y. Cheng, E. H. Sargent, and J. Tang, "Thin-film Sb_2Se_3 photovoltaics with oriented one- dimensional ribbons and benign grain boundaries," *Nat. Photonics*, 9, 409, 2015.

[7] L. Wang, D.-B. Li, K. Li, C. Chen, H.-X. Deng, L. Gao, Y. Zhao, F. Jiang, L. Li, F. Huang, Y. He, H. Song, G. Niu, and J. Tang, "Stable 6%-efficient Sb_2Se_3 solar cells with a ZnO buffer layer," *Nat. Energy*, vol. 2, no. March, p. 17046, 2017.

[8] J. Li, B. Wang, F. Liu, J. Yang, J. Li, J. Liu, M. Jia, Y. Lai, and Y. Liu, "Preparation and characterization of Bi-doped antimony selenide thin films by electrodeposition," *Electrochim. Acta*, *56*, 8597, 2011.

[9] H. Lei, G. Yang, Y. Guo, L. Xiong, P. Qin, X. Dai, X. Zheng, W. Ke, H. Tao, Z. Chen, B. Li, and G. Fang, "Efficient planar Sb_2Se_3 solar cells using a low-temperature solution-processed tin oxide electron conductor," *Phys. Chem. Chem. Phys.*, *18*, 16436, 2016.

[10] C. Chen, Y. Zhao, S. Lu, K. Li, Y. Li, B. Yang, W. Chen, L. Wang, D. Li, H. Deng, F. Yi, and J. Tang, "Accelerated optimization of TiO_2 /Sb_2Se_3 thin film solar cells by high-throughput combinatorial approach," *Adv. Energy Mater.*, vol. 1700866, p. 1700866, 2017.

[11] J. D. Major and K. Durose, "Early stage growth mechanisms of CdTe thin films deposited by close space sublimation for solar cells," *Sol. Energy Mater. Sol. Cells*, vol. 95, no. 12, pp. 3165–3170, 2011.

[12] L. J. Phillips, C. N. Savory, P. J. Yates, H. Shiel, O. S. Hutter, M. Brikett, S. Mariotti, L. Bowen, T. D. Veal, K. Durose, D. O. Scanlon, and J. D. Major, "A scalable synthesis approach to

antimony selenide solar cells," *Submitted to Nature Communications.*, 2018.

[13] O. S. Hutter, L. J. Phillips, K. Durose, and J. D. Major, "6.6% Efficient Antimony Selenide Solar Cells Using Grain Structure Control and an Organic Contact Layer," *Submitted to Solar Energy Materials Solar Cells*, 2018.

[14] T. Baines, G. Zoppi, L. Bowen, T. P. Shalvey, S. Mariotti, K. Durose, and J. D. Major, "Incorporation of CdSe layers into CdTe thin film solar cells," *Sol. Energy Mater. Sol. Cells*, vol. 180, no. February, pp. 196–204, 2018.

[15] M. Leng, M. Luo, C. Chen, S. Qin, J. Chen, J. Zhong, and J. Tang, "Optical properties of amorphous and polycrystalline Sb_2Se_3 thin films prepared by thermal evaporation," *Applied Physics Letters*, *83905*, 2015.

[16] S. Mariotti, O. S. Hutter, L. J. Phillips, P. J. Yates, B. Kundu, and K. Durose, "Stability and performance of $CsPbI_2Br$ thin films and solar cell Devices," *ACS Appl. Mater. Interfaces*, *10, 4, 3750-3760*, 2018.

[17] K. Zeng, D.-J. Xue, and J. Tang, "Antimony selenide thin-film solar cells," *Semicond. Sci. Technol.*, 31, 63001, 2016.

[18] L. Phillips, P. Yates, O. S. Hutter, T. Baines, L. Bowen, K. Durose, and J. D. Major, "Close-spaced sublimation for Sb_2Se_3 solar cells," *2017 IEEE 44rd Photovoltaic Specialists Conference (PVSC)*, 2017.

[19] J. D. Major, L. J. Phillips, M. Al Turkestani, L. Bowen, T. J. Whittles, V. R. Dhanak, and K. Durose, "P3HT as a pinhole blocking back contact for CdTe thin film solar cells," *Sol. Energy Mater. Sol. Cells*, 172, 1–10, 2017.